Title

Efficient Synthesis of Asymmetric Miktoarm Star Polymers

Journal

Macromolecules, 53(2)

ISSN

0024-9297

Authors

Levi, Adam E

Fu, Liangbing

Lequieu, Joshua

et al.

Publication Date

2020-01-28

DOI

10.1021/acs.macromol.9b02380

Peer reviewed

HHS Public Access

Author manuscript

Macromolecules. Author manuscript; available in PMC 2021 January 28.

Published in final edited form as:

Macromolecules. 2020 January 28; 53(2): 702–710. doi:10.1021/acs.macromol.9b02380.

Efficient Synthesis of Asymmetric Miktoarm Star Polymers

Adam E. Levi[†], **Liangbing Fu**[‖], **Joshua Lequieu**[‡], **Jacob D. Horne**[§], **Jacob Blankenship**[†], **Sanjoy Mukherjee**[‡], **Tianqi Zhang**[‖], **Glenn H. Fredrickson**[‡,§,⊥], **Will R. Gutekunst**[‖], **Christopher M. Bates**[⊥,†,§,*]

[†]Department of Chemistry & Biochemistry, University of California, Santa Barbara, California 93106, United States

[‡]Materials Research Laboratory, University of California, Santa Barbara, California 93106, United States

[§]Department of Chemical Engineering, University of California, Santa Barbara, California 93106, United States

[⊥]Materials Department, University of California, Santa Barbara, California 93106, United States.

[‖]School of Chemistry and Biochemistry, Georgia Institute of Technology, 901 Atlantic Drive NW, Atlanta, Georgia 30332, United States.

Abstract

Asymmetric miktoarm star polymers comprising an unequal number of chemically-distinct blocks connected at a common junction produce unique material properties, yet existing synthetic strategies are beleaguered by complicated reaction schemes that are restricted in both monomer scope and yield. Here, we introduce a new synthetic approach coined "μSTAR" — Miktoarm Synthesis by Termination After Ring-opening metathesis polymerization — that circumvents these traditional synthetic limitations by constructing the block–block junction in a scalable, one-pot process involving (1) grafting-through polymerization of a macromonomer followed by (2) *in-situ* enyne-mediated termination to install a single mikto-arm with exceptional efficiency. This modular μSTAR platform cleanly generates AB_n and $A(BA')_n$ miktoarm star polymers with unprecedented versatility in the selection of A and B chemistries as demonstrated using many common polymer building blocks: poly(siloxane), poly(acrylate), poly(methacrylate), poly(ether), poly(ester), and poly(styrene). The average number of B or BA′ arms (n) is easily controlled by the molar equivalents of macromonomer relative to Grubbs catalyst in the initial ring-opening metathesis polymerization step. While these materials are characterized by dispersity in n that arises from polymerization statistics, they self-assemble into mesophases that are identical to those predicted for precise miktoarm stars as evidenced by small-angle X-ray scattering experiments and self-consistent field theory simulations. In summary, the μSTAR technique provides a significant

[*]**Corresponding Author:** cbates@ucsb.edu.

Author Contributions

The manuscript was written by AEL, LF, WG, and CMB. Experiments were designed by AEL, LF, WG, and CMB and performed by AEL, LF, JH, JB, and TZ. Simulations were designed by JL and GHF and performed by JL. All authors have given approval to the final version of the manuscript.

The authors declare no competing financial interest.

boost in design flexibility and synthetic simplicity while retaining the salient phase behavior of precise miktoarm star materials.

Graphical Abstract

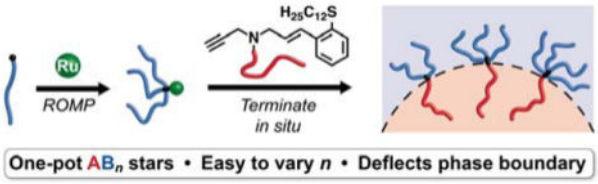

Keywords

miktoarm star; asymmetric star; polymer architecture; macromonomer; grafting-through polymerization; ring-opening metathesis polymerization; ROMP

Introduction

Block copolymers (BCPs) are important in a variety of emerging and established applications due to their self-assembly into well-ordered structures on the nanometer length scale.[1] The phase behavior of linear BCPs with two chemically-distinct blocks arrayed in simple sequences (AB, ABA, …) is now well-understood from both experiments[2–4] and theory[5–8] to depend on the Flory–Huggins interaction parameter (χ), volumetric degree of polymerization (N), block volume fractions (f_i, i = A, B), and conformational asymmetry (ε). These molecular design parameters dictate the self-assembly of two-component BCPs into a handful of classical phases[4] (body-centered cubic spheres, hexagonally close-packed cylinders, a gyroid network, lamellae) and more exotic sphere packings[9–11] (e.g., σ, C14, C15, and A15). While the utility of many such mesophases is indisputable, linear chain connectivity imposes structure–property constraints that are not always desirable. For example, the number of known morphologies remains small,[12] domain periodicities are fairly restricted (typically within a range circa 5–100 nm),[13,14] and the coupling between volume fraction (f) and morphology favors the majority block on the convex side of curved block–block interfaces.[5,15] These (and other) limitations have motivated the search for new molecular design tools that broaden the utility of BCP self-assembly in contemporary applications.

An exciting opportunity that expands the confines of traditional polymer phase behavior[16] lies in the controlled synthesis of BCPs with branched architectures.[17,18] The introduction of branching imparts useful thermodynamic,[19] photonic,[20,21] and mechanical[22] properties that are otherwise inaccessible with linear analogues. One archetypal example is miktoarm star polymers,[23–32] which are defined[33] as two or more chemically-distinct blocks connected to a common junction (e.g., A_mB_n, $m + n > 2$). The miktoarm star architecture is known or predicted to stabilize new phases,[9,15,34] reduce domain spacing,[35] and manipulate melt[25,26,36,37] or solution[38–40] properties, making them attractive for applications such as lithography and drug delivery. A further subset of miktoarm star polymers that accentuates the role of architecture in self-assembly involves asymmetry in arm number ($m \neq n$); here,

we focus on the limit $m = 1$, e.g., AB_n. As result of arm asymmetry, bulk phase boundaries are significantly deflected towards larger values of the A-block volume fraction (f_A).[5,15] This effect has been beautifully exploited by Lynd[41] and Shi[42] to design new thermoplastic elastomers ($A(BA')_n$) that are stronger, stiffer, and tougher than commercial ABA linear triblock copolymers.

Despite the importance of miktoarm star polymers in contemporary polymer science, their synthesis still remains a major challenge. The standard approach to generate precise connectivity at a common junction uses some combination of "grafting-from" and "grafting-to" multi-step reaction schemes.[43] The need for orthogonal reactivity, high yields, and designer core molecules requires tedious synthetic routes that often include time-consuming coupling, polymerization, (de)protection, and purification steps such as fractional precipitation and high performance liquid chromatography.[36,44,45] For example, the materials studied by Shi and coworkers[42] necessitated reaction times in excess of 30 days to push coupling to high conversion and still required purification via fractionation.[45–47] Moreover, changing the number of arms is non-trivial since a new core starting material must be selected each time.

Motivated by the difficulty of traditional miktoarm star polymer syntheses, we recently exploited the versatility, speed, and efficiency of Grubbs-type ring-opening metathesis polymerization (ROMP)[48–57] to synthesize miktoarm star polymers via the grafting-through copolymerization of two different macromonomers at low backbone degrees of polymerization (N_{BB}).[58] This type of statistical copolymerization is remarkably well controlled and the short backbone behaves physically like the core of a star polymer at $N_{BB} \lesssim 12$ as evidenced by experiments and theory. However, simple copolymerization trades molecular precision for synthetic versatility since the reaction stoichiometry can only control the *average* number of arms and molecular composition. As a result, bulk phase behavior is dominated by dispersity effects that counteract phase boundary deflection, even in the case of nominally asymmetric architectures. Copolymerization therefore cannot generate the unique phase behavior that distinguishes asymmetric miktoarm stars from traditional block copolymers.

Here, we introduce a new synthetic method termed μSTAR (Table 1, top) — Miktoarm Synthesis by Termination After Ring-opening metathesis polymerization — that efficiently generates asymmetric miktoarm star polymers using ruthenium-catalyzed macromonomer polymerization ($B \rightarrow B_n$) followed by *in-situ* enyne-mediated termination[59] to install the single A arm ($B_n \rightarrow AB_n$). μSTAR sits at an optimal synthetic intersection, combining the versatility and speed of a macromonomer approach using ROMP with the precision of a highly efficient coupling step. Using a handful of macromonomers and macroterminators as building blocks, a diverse library of miktoarm stars can be easily prepared with different numbers of arms and block chemistries. We highlight this modularity by synthesizing AB_n and $A(BA')_n$ miktoarm star polymers comprising six different permutations of A and B block chemistry selected from poly(siloxane), poly(acrylate), poly(methacrylate), poly(ether), poly(ester), and poly(styrene). The average number of B arms (n) is easily controlled by the equivalents of Grubbs catalyst to macromonomer in the initial polymerization step. Importantly, the phase behavior of these polymers with disperse n

exhibits significant phase boundary deflection, in agreement with self-consistent field theory (SCFT) simulations performed on precise (monodisperse *n*) analogues. A major implication of this finding is that the dispersity in *n* produced by μSTAR is advantageous from the perspective of significantly simplifying the synthesis of miktoarm star polymers while retaining the characteristic phase behavior that produces interesting bulk properties. The speed, efficiency, and broad scope of μSTAR establishes a compelling new synthetic platform for asymmetric miktoarm star polymers and supports the notion that low dispersity is not always better in block copolymer self-assembly.[60,61]

Results

Synthesis

Two types of simple linear precursors are needed in the μSTAR process to create miktoarm polymers: a macromonomer with a single polymerizable end-group and a macroterminator that will irreversibly couple exactly once to the active chain ends. We focus on using Grubbs-type ring-opening metathesis polymerization (ROMP) to construct the junction due to its well-established functional group tolerance, fast reaction rates, and high yields.[62] Norbornene was therefore selected as the polymerizable group on the macromonomer because it undergoes efficient ROMP;[63] both homopolymer (B) and diblocks (BA′) will be discussed with norbornene installed on the B terminus. For the macroterminator, we exploit enyne-mediated termination chemistry recently developed by Gutekunst and coworkers[59] to perform macromolecular coupling of living metathesis polymers.[64,65] While enyne macroterminators were previously shown to efficiently prepare diblocks, the sterics involved in coupling to the core of a star polymer present a unique challenge.[66] Nevertheless, the high reactivity of enynes makes them suitable for macromolecular couplings that would otherwise not be possible with traditional ROMP termination methods employing substituted vinyl ethers or symmetrical *cis*-olefins.[67–71] The generic end-groups used in μSTAR are illustrated in Table 1 (top).

Macromonomers with different B chemistry were synthesized by polymerization from functional norbornene initiators or coupling reactions between a norbornene acid and commercially available monotelechelic polymers. In summary, six different macromonomers were synthesized that span various classes of polymer chemistry: poly(lactide) (PLA), poly(dimethylsiloxane) (PDMS), poly(4-methylcaprolactone–*block*–lactide) (PMCL-PLA), poly(styrene) (PS), poly(2-trifluoroethyl acrylate) (PTFEA), and poly(methyl methacrylate) (PMMA). Similarly, six macroterminators (A) were prepared by coupling to or directly growing from the enyne terminator molecule. PDMS, PLA, poly(ethylene oxide) (PEO), poly(*n*-butyl acrylate) (PnBA), and poly(*tert*-butyl acrylate) (PtBA) were chosen as the A block (see Supporting Information). The methyl ester enyne small molecule can be prepared in four high yielding steps and is further derivatized into the terminator of choice by one or two additional reactions.[59] Table 1 (bottom) summarizes these materials; full characterization details are provided in the Supporting Information (Tables S1–S2, Figure S1).

The efficacy of μSTAR at synthesizing asymmetric miktoarm star polymers is evident in Figure 1, which summarizes size-exclusion chromatograms (SECs) of the macromonomers

(dashed lines), macroterminators (dashed lines), and resultant miktoarm star polymers (solid lines) for the combinations described in Table 1. The general process involves two steps that occur in one pot. (1) Polymerization of the macromonomer creates a short bottlebrush (N_{BB} < 12) with star-like physical properties[58] (*vide infra*); after complete conversion, an aliquot of the poly(macromonomer) is extracted. (2) *In situ* termination by the addition of macroterminator efficiently couples a single A arm to the living star polymer, resulting in AB_n or $A(BA')_n$ chain connectivity. SEC traces of the poly(macromonomers) are omitted from Figure 1 for clarity but can be found in Figures S2–S10. Note that with the exception of Figure 1f, $n = 4$ was targeted in this initial set of examples. Kinetic experiments performed with a model 5 kDa PLA macroterminator indicate the coupling process is finished in about 2 hours at room temperature (Figure S11). After termination, the increase in poly(macromonomer) absolute molecular weight as measured with multi-angle light scattering (MALS) is consistent with the macroterminator size (Table S3–S4). A single precipitation into methanol, diethyl ether, or hexanes is sufficient to isolate the final miktoarm star polymers, which have low molar mass dispersities ($Đ < 1.2$, Table S4) and monomodal SEC traces (Figure 1). ^{1}H nuclear magnetic resonance (NMR) measurements further confirmed the stoichiometric coupling of macroterminator and poly(macromonomer) (Figure S12–S22) and were also used to calculate compositions as tabulated in Table S4. Diffusion-ordered spectroscopy (DOSY) analysis revealed that these miktoarm star polymers lack homopolymer contamination within measurement error (Tables S5–S6, Figure S23–S24)[72] as attempts to determine the percent of homopolymer contamination with multi-component fits yielded inconsistent results and non-physical diffusion coefficients, which is evidence of data overfitting.[73]

Another advantage of μSTAR is the ability to easily vary the average number of B or BA′ arms by changing the equivalents of macromonomer to Grubbs initiator. A series of four $A(BA')_n$ asymmetric miktoarm star polymers (A = PLA, BA′ = PMCL–*block*–PLA) with n = 3, 5, 7, or 9 arms was prepared simultaneously in separate reaction vessels using the same macromonomer and macroterminator precursors (Figure 2). SEC traces smoothly decrease in elution time as n increases, and absolute molecular weight measurements are consistent with increasing the average number of poly(macromonomer) arms across the range $n = 3 – 9$ (Table S3). This ability to easily vary the number of arms stands in stark contrast to all previous synthetic strategies where a different initiator or core must be synthesized whenever the number of arms is varied.[29,45,74] These materials also highlight the tolerance of μSTAR chemistry to high molecular weights; for $n = 9$, a 54 kDa poly(macromonomer) cleanly couples to a 24 kDa PLA macroterminator using only 1.1 equivalents of the latter.

Self-Assembly

A key question that remains is whether asymmetric miktoarm star polymers synthesized via μSTAR (with dispersity in n) self-assemble as predicted by theory for precise analogues. We have opted to study in detail the phase behavior of the $(PLA\text{-}PMCL)_n$-PLA samples described in Figures 1 and 2 since the addition of a short A′ block flanking B is predicted to further accentuate the phase boundary deflections that are characteristic of asymmetric AB_n miktoarm star polymers.[41] Figure 3a reports synchrotron small angle X-ray scattering (SAXS) patterns collected at room temperature after annealing $(PLA\text{-}PMCL)_n$-PLA with a

varying number of PLA-PMCL diblock arms (n = 3 – 9) at 140 °C for 18 hours. Note that the volume fraction of PLA (f_{PLA}) changes with n such that these samples span f_{PLA} = 0.58 – 0.71. The SAXS traces for n = 3 (f_{PLA} = 0.71), n = 5 (f_{PLA} = 0.68), and n = 7 (f_{PLA} = 0.62) can be cleanly indexed as indicated by triangles that demarcate the expected location of scattering reflections for lamellar (LAM), gyroid (GYR), and hexagonally close-packed cylinders (HEX), respectively. The n = 9 material shows broader peaks that are less well-defined, but their intensity maxima roughly coincide with those expected for a spherical form factor and Percus–Yevick structure factor[75] (Figure S25); we tentatively ascribe this morphology as disordered spheres that possibly fail to order on a well-defined lattice due to kinetic limitations. Collectively, these data are consistent with a remarkable deflection of order–order phase boundaries towards larger f_A relative to linear AB diblock or ABA triblock copolymers. For example, the HEX–GYR transition occurs near f_A = 0.3 with linear diblocks versus in the vicinity of f_A = 0.62 – 0.68 that we measure for (PLA-PMCL)$_n$-PLA mikto polymers. We are confident that the PLA block resides in the interior of the cylinders since GYR (f_{PLA} = 0.68) and LAM (f_{PLA} = 0.71) occur at even larger volume fractions. Perhaps stronger direct proof is the HEX sample exhibits recoverable elasticity in cyclic tensile tests, the details of which will be described in a forthcoming report. These experimental data relating morphology and volume fraction are in agreement with SCFT simulations performed on A(BA′)$_n$ asymmetric miktoarm star polymers using the literature-reported[76] value of $\chi_{PLA–PMCL}$ and the degrees of polymerization measured experimentally for A = PLA and BA′ = PMCL-PLA (Figure 3b, see Supporting Information for details). We conclude that asymmetric miktoarm star polymers synthesized via μSTAR — which necessarily have dispersity in n — can self-assemble into structures that mimic precise molecular analogues.

Discussion

Historically, anionic polymerization has been the workhorse synthetic technique used to construct miktoarm star polymers, including AB$_n$[32,66,77–79] and A(BA′)$_n$[42,45] asymmetric variants. While effective, rigorous purification requirements, a limited monomer scope, sequence constraints, sluggish coupling kinetics[47] (that can take months to reach full conversion), and the need for additional purification by fractional precipitation[32,45,78] are inconvenient from both practical and design perspectives. μSTAR overcomes all of these challenges, assuming that dispersity in n can be tolerated, by exploiting the well-established functional group compatibility and speed of ROMP. We note that a conceptually similar approach has been attempted with anionic polymerization in the past, namely the grafting-through polymerization of a polystyrene (polyisoprene) macromonomer to construct the B$_n$ core, either preceded or followed by the polymerization of polyisoprene (polystyrene) to grow a single A block.[80] The result was rather broad and multimodal SEC traces, particularly for the poly(macromonomers). Despite improvement after repeated fractional precipitation, even a further optimized anionic methodology would lack the versatility of a ROMP-based approach.

The examples in Figures 1 and 2 were selected to accentuate different types of chemistry that are of contemporary importance and challenging to link together using traditional miktoarm star syntheses. For example, PLA$_n$-PDMS (Figure 1a) and PDMS$_n$-PLA (Figure

1b) may be useful as lithographic materials with higher resolution than linear analogues due to architecture effects while maintaining good etch contrast.[13,19,35,37,81,82] In the field of electrochemical energy storage, miktoarm star polymers containing PEO blocks are of interest as safe battery electrolytes, yet their reported synthesis is involved.[36] We have demonstrated that PS_n-PEO miktoarm stars are straightforward to synthesize with μSTAR (Figure 1c). μSTAR also provides access to amphiphilic miktoarm star polymers, e.g., by combining a PMMA macromonomer and PtBA terminator (Figure 1d) followed by acid-catalyzed deprotection of the *tert*-butyl ester to poly(acrylic acid) (PAA). The sulfonamide–pyrroline linkage created during termination is robust enough withstand a concentrated solution of trifluoroacetic acid and yield the partially charged $PMMA_n$-PAA star polymer (Figure S26–S29). Figure 1e further showcases a combination of acrylates ($PTFEA_4$-PnBA) that would be especially difficult to access via a core-first approach since both monomers undergo polymerization with the same type of radical initiator; the incorporation of semi-fluorinated acrylates may also create opportunities in surface coatings and other advanced materials.[83–86]

As introduced earlier, the $A(BA')_n$ architecture presents exciting opportunities for next-generation thermoplastic elastomers.[42] To date, this concept has only been explored using A, A′ = poly(styrene) (PS) and B = poly(isoprene) (PI) blocks synthesized by anionic polymerization and silyl chloride coupling.[45] Inspired by the work of Hillmyer,[76] here we have shown that renewable types of glassy (PLA) and rubbery (PMCL) polyesters can form $A(BA')_n$ miktoarm stars with $n = 3 – 9$ using μSTAR (Figure 1f), which are inaccessible via the established anionic route. The phase behavior of $(PLA\text{-}PMCL)_n$-PLA asymmetric miktoarm star polymers synthesized with μSTAR is consistent with past experimental reports on precise $(PS\text{-}PI)_3$-PS[42] and theory that anticipate significant deflection of order–order transitions towards larger volume fractions due to molecular architecture. We have not observed this effect in any simple ROMP copolymerizations involving A and B macromonomers,[58] even at unequal feed compositions, which suggests that efficient termination chemistry (or some other method of installing a single A arm) is key to unlocking the unique self-assembly of asymmetric miktoarm star polymers. This result bolsters our previous finding that short bottlebrushes actually behave like miktoarm star polymers despite the inherent dispersity in n.[58] Note that SCFT simulations reveal a large sensitivity to the relative lengths of A and A′ blocks as parameterized by $\tau = N_A/(N_A+N_{A'})$ (Figure S30). Although our experimental calculation of τ is based on molar masses measured by NMR ($\tau = 0.896$) and MALS ($\tau = 0.925$) that are within reasonable experimental uncertainty, SCFT simulations match the data in Figure 3a best with an intermediate $\tau = 0.91$ shown in Figure 3b. SCFT also accurately captures the temperature-dependent phase behavior of these materials. By measuring the order–disorder transition temperature (T_{ODT}) with variable temperature SAXS (Figure S31) and calculating $\chi(T_{ODT})$ from the relationship reported by Watts,[76] $(\chi N)_{ODT}$ was compared to SCFT predictions. Incredibly, for $n = 3$, the theoretical and experimental values differ by less than 1% (Figure S32). As n increases, the deviation grows, but it never exceeds 12%.

We hasten to note that not all miktoarm star samples produced with μSTAR show scattering reflections that are as well-resolved as those in Figure 3. This may be the result of thermodynamic or kinetic factors that are influenced by architecture, dispersity, high

molecular weight, or a combination thereof. For example, with $n = 9$ and $f_A = 0.58$ (Figure 3a), the thermodynamically stable phase might be A15,[15,87] which is likely kinetically inaccessible above a certain threshold molecular weight.[88] Another possibility is a complex free energy landscape; Grason and coworkers have previously argued that kinetic trapping could cause a similar glassy intermediate phase in AB_2 miktoarm stars due to the near degeneracy of BCC and A15.[15] Thus, it is not surprising that complex sphere phase formation is suppressed.[10,88] Nevertheless, we find it remarkable that μSTAR can produce clean self-assembly given the dispersity in n.

Figure 4 illustrates the key differences in molecular composition and self-assembly that result from various miktoarm star synthesis techniques. Simple ROMP copolymerization with either a blocky or statistical sequence at low N_{BB} generates composition and arm-number dispersity that together tend to favor a flat block–block interface (Figure 4a).[58] At the same overall composition (i.e., $f_A = 0.5$), asymmetric miktoarm star polymers with a precise number of arms (for example, AB_3) bias interfacial curvature toward the A block (Figure 4b).[15,26] Samples synthesized using μSTAR sit somewhere in between — exactly one A arm and a distribution of B arms still results in self-assembly that favors interfacial curvature, the magnitude of which is evidently similar to precise analogues with the average μSTAR composition (Figure 4c). One benefit of incorporating such dispersity lies in relaxing the synthetic burden without drastically impacting self-assembly.

Conclusion

In summary, we have introduced a new synthetic technique termed μSTAR that generates AB_n and $A(BA')_n$ asymmetric miktoarm star polymers using grafting-through polymerization and efficient enyne-mediated polymer–polymer coupling chemistry. This modular approach is compatible with a wide variety of polymer chemistries and can accommodate high molecular weight arms. The average number of B or BA′ arms (n) is easily varied by the ratio of Grubbs catalyst to macromonomer in the initial polymerization step. Miktoarm star polymers made via μSTAR exhibit large deflections in the block copolymer phase diagram (relative to linear analogues) unlike stars produced by statistical grafting-through copolymerization. Despite the dispersity in n, experimental phase behavior matches SCFT calculations performed with precise molecular connectivity. μSTAR significantly simplifies the synthesis of asymmetric miktoarm star polymers when dispersity in arm number can be tolerated.

Supplementary Material

Refer to Web version on PubMed Central for supplementary material.

Acknowledgments

The authors thank Craig J. Hawker and his group for helpful discussions. The authors also thank Dr. Rachel Behrens (UCSB) and Dr. Cheng Zhang for assistance in polymer characterization and analysis. X-ray scattering experiments were performed at the Advanced Light Source (a U.S. Department of Energy (DOE) Office of Science User Facility, DE-AC02-05CH11231; beamline 7.3.3), the Stanford Synchrotron Radiation Lightsource (supported by the U.S. DOE Office of Science, Office of Basic Energy Sciences, DEAC02-76SF00515; beamline 1-5).

Funding Sources

This material is based upon work supported by the U.S. Department of Energy, Office of Basic Energy Sciences, under Award Number DE-SC0019001. AEL and JB thank the Mellichamp Academic Initiative in Sustainability for summer fellowships. WRG acknowledges the Georgia Institute of Technology for start-up funds and the National Institutes of Health under Award Number R35GM133784. The research reported here made use of shared facilities of the UCSB NSF MRSEC (DMR-1720256), a member of the Materials Research Facilities Network (www.mrfn.org). We also acknowledge support from the Center for Scientific Computing from the CNSI, MRL: an NSF MRSEC (DMR-1720256) and NSF CNS-1725797.

References

(1). Bates FS; Hillmyer MA; Lodge TP; Bates CM; Delaney KT; Fredrickson GH Multiblock Polymers: Panacea or Pandora's Box? Science 2012, 336, 434–440. [PubMed: 22539713]

(2). Hajduk DA; Harper PE; Gruner SM; Honeker CC; Kim G; Fetters LJ; Kim G The Gyroid: A New Equilibrium Morphology in Weakly Segregated Diblock Copolymers. Macromolecules 1994, 27, 4063–4075.

(3). Bates FS; Schulz MF; Khandpur AK; Förster S; Rosedale JH; Almdal K; Mortensen K Fluctuations, Conformational Asymmetry and Block Copolymer Phase Behaviour. Faraday Discuss. 1994, 98, 7–18.

(4). Bates F Block Copolymer Thermodynamics: Theory And Experiment. Annu. Rev. Phys. Chem 1990, 41, 525–557. [PubMed: 20462355]

(5). Milner ST Chain Architecture and Asymmetry in Copolymer Microphases. Macromolecules 1994, 27, 2333–2335.

(6). Leibler L Theory of Microphase Separation in Block Copolymers. Macromolecules 1980, 13, 1602–1617.

(7). Matsen MW; Schick M Stable and Unstable Phases of a Diblock Copolymer Melt. Phys. Rev. Lett 1994, 72, 2660–2663. [PubMed: 10055940]

(8). Matsen MW; Bates FS Unifying Weak- and Strong-Segregation Block Copolymer Theories. Macromolecules 1996, 29, 1091–1098.

(9). Li W; Duan C; Shi AC Nonclassical Spherical Packing Phases Self-Assembled from AB-Type Block Copolymers. ACS Macro Lett. 2017, 6, 1257–1262.

(10). Bates MW; Lequieu J; Barbon SM; Lewis RM; Delaney KT; Anastasaki A; Hawker CJ; Fredrickson GH; Bates CM Stability of the A15 Phase in Diblock Copolymer Melts. Proc. Natl. Acad. Sci 2019, 116, 13194–13199. [PubMed: 31209038]

(11). Kim K; Schulze MW; Arora A; Lewis RM; Marc A; Dorfman KD; Bates FS Thermal Processing of Diblock Copolymer Melts Mimics Metallurgy. Science 2017, 356, 520–523. [PubMed: 28473585]

(12). Bates CM; Bates FS 50th Anniversary Perspective: Block Polymers-Pure Potential. Macromolecules 2017, 50, 3–22.

(13). Sinturel C; Bates FS; Hillmyer MA High χ-Low N Block Polymers: How Far Can We Go? ACS Macro Lett. 2015, 4, 1044–1050.

(14). Jeong SJ; Kim JY; Kim BH; Moon HS; Kim SO Directed Self-Assembly of Block Copolymers for next Generation Nanolithography. Mater. Today 2013, 16, 468–476.

(15). Grason GM; Kamien RD Interfaces in Diblocks: A Study of Miktoarm Star Copolymers. Macromolecules 2004, 37, 7371–7380.

(16). Bates FS Polymer-Polymer Phase Behavior. Science 1991, 251, 898. [PubMed: 17847383]

(17). Le AN; Liang R; Zhong M Synthesis and Self-Assembly of Mixed-Graft Block Copolymers. Chem. - A Eur. J 2019, 25, 8177–8189.

(18). Polymeropoulos G; Zapsas G; Ntetsikas K; Bilalis P; Gnanou Y; Hadjichristidis N 50th Anniversary Perspective: Polymers with Complex Architectures. Macromolecules 2017, 50, 1253–1290.

(19). Guo Z; Le AN; Feng X; Choo Y; Liu B; Wang D; Wan Z; Gu Y; Zhao J; Li V; Osuji CO; Johnson JA; Zhong M Janus Graft Block Copolymers: Design of Polymer Architecture for Independently Tuned Nanostructures and Polymer Properties. Angew. Chem. Int. Ed 2018, 57, 8493–8497.

(20). Sveinbjornsson BR; Weitekamp RA; Miyake GM; Xia Y; Atwater HA; Grubbs RH Rapid Self-Assembly of Brush Block Copolymers to Photonic Crystals. Proc. Natl. Acad. Sci 2012, 109, 14332–14336. [PubMed: 22912408]

(21). Vatankhah-Varnosfaderani M; Keith AN; Cong Y; Liang H; Rosenthal M; Sztucki M; Clair C; Magonov S; Ivanov DA; Dobrynin AV; Sheiko SS Chameleon-like Elastomers with Molecularly Encoded Strain-Adaptive Stiffening and Coloration. Science 2018, 359, 1509–1513. [PubMed: 29599240]

(22). Wang H; Lu W; Wang W; Shah PN; Misichronis K; Kang NG; Mays JW Design and Synthesis of Multigraft Copolymer Thermoplastic Elastomers: Superelastomers. Macromol. Chem. Phys 2018, 219, 1–11.

(23). Li Z; Kesselman E; Talmon Y; Hillmyer MA; Lodge TP Multicompartment Micelles from ABC Miktoarm Stars in Water. Science 2004, 306, 98–101. [PubMed: 15459387]

(24). Miktoarm Star Polymers: From Basics of Branched Architecture to Synthesis, Self-Assembly and Applications; Kakkar A, Ed.; The Royal Society of Chemistry, 2017.

(25). Yang L; Hong S; Gido SP; Velis G; Hadjichristidis N I5S Miktoarm Star Block Copolymers: Packing Constraints on Morphology and Discontinuous Chevron Tilt Grain Boundaries. Macromolecules 2001, 34, 9069–9073.

(26). Beyer FL; Gido SP; Velis G; Hadjichristidis N; Tan NB Morphological Behavior of A5B Miktoarm Star Block Copolymers. Macromolecules 1999, 32, 6604–6607.

(27). Pochan DJ; Gido SP; Pispas S; Mays JW Morphological Transitions in an I2S Simple Graft Block Copolymer: From Folded Sheets to Folded Lace to Randomly Oriented Worms at Equilibrium. Macromolecules 1996, 29, 5099–5105.

(28). Pochan DJ; Gido SP; Zhou J; Mays JW; Whitmore M; Ryan AJ Morphologies of Microphase-separated Conformationally Asymmetric Diblock Copolymers. J. Polym. Sci. Part B Polym. Phys 1997, 35, 2629–2643.

(29). Beyer FL; Gido SP; Poulos Y; Avgeropoulos A; Hadjichristidis N Morphology of Vergina Star 16-Arm Block Copolymers and Scaling Behavior of Interfacial Area with Graft Point Functionality. Macromolecules 1997, 30, 2373–2376.

(30). Gido SP; Lee C; Pochan DJ; Pispas S; Mays JW; Hadjichristidis N Synthesis, Characterization, and Morphology of Model Graft Copolymers with Trifunctional Branch Points. Macromolecules 1996, 29, 7022–7028.

(31). Hadjichristidis N; Iatrou H; Behal SK; Chludzinski JJ; Disko MM; Garner RT; Liang KS; Lohse DJ; Milner ST Morphology and Miscibility of Miktoarm Styrene-Diene Copolymers and Terpolymers. Macromolecules 1993, 26, 5812–5815.

(32). Tselikas Y; Iatrou H; Hadjichristidis N; Liang KS; Mohanty K; Lohse DJ Morphology of Miktoarm Star Block Copolymers of Styrene and Isoprene. J. Chem. Phys 1996, 105, 2456–2462.

(33). Iatrou H; Hadjichristidis N Synthesis and Characterization of Model 4-Miktoarm Star Co- and Quaterpolymers. Macromolecules 1993, 26, 2479–2484.

(34). Aissou K; Choi HK; Nunns A; Manners I; Ross CA Ordered Nanoscale Archimedean Tilings of a Templated 3-Miktoarm Star Terpolymer. Nano Lett. 2013, 13, 835–839. [PubMed: 23343324]

(35). Shi W; Tateishi Y; Li W; Hawker CJ; Fredrickson GH; Kramer EJ Producing Small Domain Features Using Miktoarm Block Copolymers with Large Interaction Parameters. ACS Macro Lett. 2015, 4, 1287–1292.

(36). Lee D; Jung HY; Park MJ Solid-State Polymer Electrolytes Based on AB3-Type Miktoarm Star Copolymers. ACS Macro Lett. 2018, 7, 1046–1050.

(37). Minehara H; Pitet LM; Kim S; Zha RH; Meijer EW; Hawker CJ Branched Block Copolymers for Tuning of Morphology and Feature Size in Thin Film Nanolithography. Macromolecules 2016, 49, 2318–2326.

(38). Kakkar A; Traverso G; Farokhzad OC; Weissleder R; Langer R Evolution of Macromolecular Complexity in Drug Delivery Systems. Nat. Rev. Chem 2017, 1, 1–17.

(39). Lin W; Nie S; Zhong Q; Yang Y; Cai C; Wang J; Zhang L Amphiphilic Miktoarm Star Copolymer (PCL)3-(PDEAEMA-b-PPEGMA)3 as PH-Sensitive Micelles in the Delivery of Anticancer Drug. J. Mater. Chem. B 2014, 2, 4008–4020. [PubMed: 32261652]

(40). Gelissen APH; Pergushov DV; Plamper FA Janus-like Interpolyelectrolyte Complexes Based on Miktoarm Stars. Polymer (Guildf). 2013, 54, 6877–6881.

(41). Lynd NA; Oyerokun FT; O'Donoghue DL; Handlin DL; Fredrickson GH Design of Soft and Strong Thermoplastic Elastomers Based on Nonlinear Block Copolymer Architectures Using Self-Consistent-Field Theory. Macromolecules 2010, 43, 3479–3486.

(42). Shi W; Lynd NA; Montarnal D; Luo Y; Fredrickson GH; Kramer EJ; Ntaras C; Avgeropoulos A; Hexemer A Toward Strong Thermoplastic Elastomers with Asymmetric Miktoarm Block Copolymer Architectures. Macromolecules 2014, 47, 2037–2043.

(43). Ren JM; McKenzie TG; Fu Q; Wong EHH; Xu J; An Z; Shanmugam S; Davis TP; Boyer C; Qiao GG Star Polymers. Chem. Rev 2016, 116, 6743–6836. [PubMed: 27299693]

(44). Liu H; Pan W; Tong M; Zhao Y Synthesis and Properties of Couplable ABCDE Star Copolymers by Orthogonal CuAAC and Diels-Alder Click Reactions. Polym. Chem 2016, 7, 1603–1611.

(45). Avgeropoulos A; Hadjichristidis N; Copolymer SB Synthesis of Model Nonlinear Block Copolymers of A(BA)2, A(BA)3, and (AB)3A(BA)3 Type. J. Polym. Sci. Part A Polym. Chem 1997, 35, 813–816.

(46). Avgeropoulos A; Dair BJ; Hadjichristidis N; Thomas EL Tricontinuous Double Gyroid Cubic Phase in Triblock Copolymers of the ABA Type. 1997, 9297, 5634–5642.

(47). Zhu Y; Gido SP; Moshakou M; Iatrou H; Hadjichristidis N; Park S; Chang T Effect of Junction Point Functionality on the Lamellar Spacing of Symmetric (PS)n(PI)n Miktoarm Star Block Copolymers. Macromolecules 2003, 36, 5719–5724.

(48). Shibuya Y; Nguyen HVT; Johnson JA Mikto-Brush-Arm Star Polymers via Cross-Linking of Dissimilar Bottlebrushes: Synthesis and Solution Morphologies. ACS Macro Lett. 2017, 6, 963–968.

(49). Burts AO; Gao AX; Johnson JA Brush-First Synthesis of Core-Photodegradable Miktoarm Star Polymers via ROMP: Towards Photoresponsive Self-Assemblies. Macromol. Rapid Commun 2014, 35, 168–173. [PubMed: 24265215]

(50). Gorodetskaya IA; Choi TL; Grubbs RH Hyperbranched Macromolecules via Olefin Metathesis. J. Am. Chem. Soc 2007, 129, 12672–12673. [PubMed: 17902678]

(51). Liu J; Burts AO; Li Y; Zhukhovitskiy AV; Ottaviani MF; Turro NJ; Johnson JA "Brush-First" Method for the Parallel Synthesis of Photocleavable, Nitroxide-Labeled Poly(Ethylene Glycol) Star Polymers. J. Am. Chem. Soc 2012, 134, 16337–16344. [PubMed: 22953714]

(52). Dutertre F; Bang KT; Vereroudakis E; Loppinet B; Yang S; Kang SY; Fytas G; Choi TL Conformation of Tunable Nanocylinders: Up to Sixth-Generation Dendronized Polymers via Graft-Through Approach by ROMP. Macromolecules 2019, 52, 3342–3350. [PubMed: 31496546]

(53). Xia Y; Olsen BD; Kornfield JA; Grubbs RH Efficient Synthesis of Narrowly Dispersed Brush Copolymers and Study of Their Assemblies: The Importance of Side Chain Arrangement. J. Am. Chem. Soc 2009, 131, 18525–18532. [PubMed: 19947607]

(54). Xia Y; Grubbs RH Efficient Syntheses of Brush Polymers via Living Ring Opening Metathesis Polymerization of Macromonomers. Macromolecules 2009, 50, 197–198.

(55). Teo YC; Xia Y Facile Synthesis of Macromonomers via ATRP-Nitroxide Radical Coupling and Well-Controlled Brush Block Copolymers. Macromolecules 2019, 52, 81–87.

(56). Walsh DJ; Guironnet D Macromolecules with Programmable Shape, Size, and Chemistry. Proc. Natl. Acad. Sci. U. S. A 2019, 116, 1538–1542. [PubMed: 30655343]

(57). Kawamoto K; Zhong M; Gadelrab KR; Cheng LC; Ross CA; Alexander-Katz A; Johnson JA Graft-through Synthesis and Assembly of Janus Bottlebrush Polymers from A-Branch-B Diblock Macromonomers. J. Am. Chem. Soc 2016, 138, 11501–11504. [PubMed: 27580971]

(58). Levi AE; Lequieu J; Horne JD; Bates MW; Ren JM; Delaney KT; Fredrickson GH; Bates CM Miktoarm Stars via Grafting-Through Copolymerization: Self-Assembly and the Star-to-Bottlebrush Transition. Macromolecules 2019, 52, 1794–1802.

(59). Fu L; Zhang T; Fu G; Gutekunst WR Relay Conjugation of Living Metathesis Polymers. J. Am. Chem. Soc 2018, 140, 12181–12188. [PubMed: 30160479]

(60). Lutz J-F; Ouchi M; Liu DR; Sawamoto M Sequence-Controlled Polymers. Science 2013, 341, 1238149. [PubMed: 23929982]

(61). Widin JM; Schmitt AK; Schmitt AL; Im K; Mahanthappa MK Unexpected Consequences of Block Polydispersity on the Self-Assembly of ABA Triblock Copolymers. J. Am. Chem. Soc 2012, 134, 3834–3844. [PubMed: 22280467]

(62). Ogba OM; Warner NC; O'Leary DJ; Grubbs RH Recent Advances in Ruthenium-Based Olefin Metathesis. Chem. Soc. Rev 2018, 47, 4510–4544. [PubMed: 29714397]

(63). Jha S; Dutta S; Bowden NB Synthesis of Ultralarge Molecular Weight Bottlebrush Polymers Using Grubbs' Catalysts. Macromolecules 2004, 37, 4365–4374.

(64). Elling BR; Xia Y Efficient and Facile End Group Control of Living Ring-Opening Metathesis Polymers via Single Addition of Functional Cyclopropenes. ACS Macro Lett. 2018, 7, 656–661.

(65). Elling BR; Su JK; Feist JD; Xia Y Precise Placement of Single Monomer Units in Living Ring-Opening Metathesis Polymerization. Chem 2019, 1–11.

(66). Mavroudis A; Avgeropoulos A; Hadjichristidis N; Thomas EL; Lohse DJ Synthesis and Morphological Behavior of Model Linear and Miktoarm Star Copolymers of 2-Methyl-1,3-Pentadiene and Styrene. Chem. Mater 2003, 15, 1976–1983.

(67). Matson JB; Grubbs RH Monotelechelic Poly(Oxa)Norbornenes by Ring-Opening Metathesis Polymerization Using Direct End-Capping and Cross-Metathesis. Macromolecules 2010, 43, 213–221. [PubMed: 20871800]

(68). Hilf S; Kilbinger AFM Thiol-Functionalized ROMP Polymers via Sacrificial Synthesis. Macromolecules 2009, 42, 4127–4133.

(69). Hilf S; Grubbs RH; Kilbinger AFM End Capping Ring-Opening Olefin Metathesis Polymerization Polymers with Vinyl Lactones. J. Am. Chem. Soc 2008, 130, 11040–11048. [PubMed: 18646851]

(70). Gordon EJ; Gestwicki JE; Strong LE; Kiessling LL Synthesis of End-Labeled Multivalent Ligands for Exploring Cell-Surface-Receptor-Ligand Interactions. Chem. Biol 2000, 7, 9–16. [PubMed: 10662681]

(71). Hilf S; Kilbinger AFM Functional End Groups for Polymers Prepared Using Ring-Opening Metathesis Polymerization. Nat. Chem 2009, 1, 537–546. [PubMed: 21378934]

(72). Yu Q; Pichugin D; Cruz M; Guerin G; Manners I; Winnik MA NMR Study of the Dissolution of Core-Crystalline Micelles. Macromolecules 2018, 51, 3279–3289.

(73). Gauch Hugh G.. Prediction, Parsimony and Noise. Am. Sci 1993, 81, 468–478.

(74). Isoprene I; Velis G; Hadjichristidis N Synthesis of Model PS(PI) 5 and (PI) 5 PS(PI) 5 Nonlinear Block Copolymers of Styrene (S) and Isoprene (I). 1999, 534–536.

(75). Bates CM; Chang AB; Schulze MW; Momčilovic N; Jones SC; Grubbs RH Brush Polymer Ion Gels. J. Polym. Sci. Part B Polym. Phys 2016, 54, 292–300.

(76). Watts A; Kurokawa N; Hillmyer MA Strong, Resilient, and Sustainable Aliphatic Polyester Thermoplastic Elastomers. Biomacromolecules 2017, 18, 1845–1854. [PubMed: 28467049]

(77). Lee C; Gido SP; Pitsikalis M; Mays JW; Tan NB; Trevino SF; Hadjichristidis N Asymmetric Single Graft Block Copolymers: Effect of Molecular Architecture on Morphology. Macromolecules 1997, 30, 3732–3738.

(78). Velis G; Hadjichristidis N Synthesis of Model PS(PI)5 and (PI)5PS(PI)5 Nonlinear Block Copolymers of Styrene (S) and Isoprene (I). Macromolecules 1999, 32, 534–536.

(79). Iatrou H; Siakali-Kioulafa E; Hadjichristidis N; Roovers J; Mays J Hydrodynamic Properties of Model 3-miktoarm Star Copolymers. J. Polym. Sci. Part B Polym. Phys 1995, 33, 1925–1932.

(80). Se K; Hayashino Y Anionic Living Polymerization of Macromonomers : Preparation of (A)n-Star-(B)1 Star Block Copolymers and Some Properties of the Products Obtained. Macromolecules 2007, 40, 429–437.

(81). Rodwogin MD; Spanjers CS; Leighton C; Hillmyer MA Polylactide-Poly(Dimethylsiloxane)-Polylactide Triblock Copolymers as Multifunctional Materials for Nanolithographic Applications. ACS Nano 2010, 4, 725–732. [PubMed: 20112923]

(82). Pitet LM; Wuister SF; Peeters E; Kramer EJ; Hawker CJ; Meijer EW Well-Organized Dense Arrays of Nanodomains in Thin Films of Poly(Dimethylsiloxane)-b-Poly(Lactide) Diblock Copolymers. Macromolecules 2013, 46, 8289–8295.

(83). Kassis CM; Steehler JK; Betts DE; Guan Z; Romack TJ; DeSimone JM; Linton RW XPS Studies of Fluorinated Acrylate Polymers and Block Copolymers with Polystyrene. Macromolecules 1996, 29, 3247–3254.

(84). Zhang J; Clark MB; Wu C; Li M; Trefonas P; Hustad PD Orientation Control in Thin Films of a High-χ Block Copolymer with a Surface Active Embedded Neutral Layer. Nano Lett. 2016, 16, 728–735. [PubMed: 26682931]

(85). Morita M; Ogisu H; Kubo M Surface Properties of Perfluoroalkylethyl Acrylate / n-Alkyl. J. Appl. Polym. Sci 1998, No. 2, 1741–1749.

(86). Fu C; Zhang C; Peng H; Han F; Baker C; Wu Y; Ta H; Whittaker AK Enhanced Performance of Polymeric 19F MRI Contrast Agents through Incorporation of Highly Water-Soluble Monomer MSEA. Macromolecules 2018, 51, 5875–5882.

(87). Xie N; Li W; Qiu F; Shi AC σ Phase Formed in Conformationally Asymmetric AB-Type Block Copolymers. ACS Macro Lett. 2014, 3, 909–910.

(88). Lewis RM; Arora A; Beech HK; Lee B; Lindsay AP; Lodge TP; Dorfman KD; Bates FS Role of Chain Length in the Formation of Frank-Kasper Phases in Diblock Copolymers. Phys. Rev. Lett 2018, 121, 208002. [PubMed: 30500248]

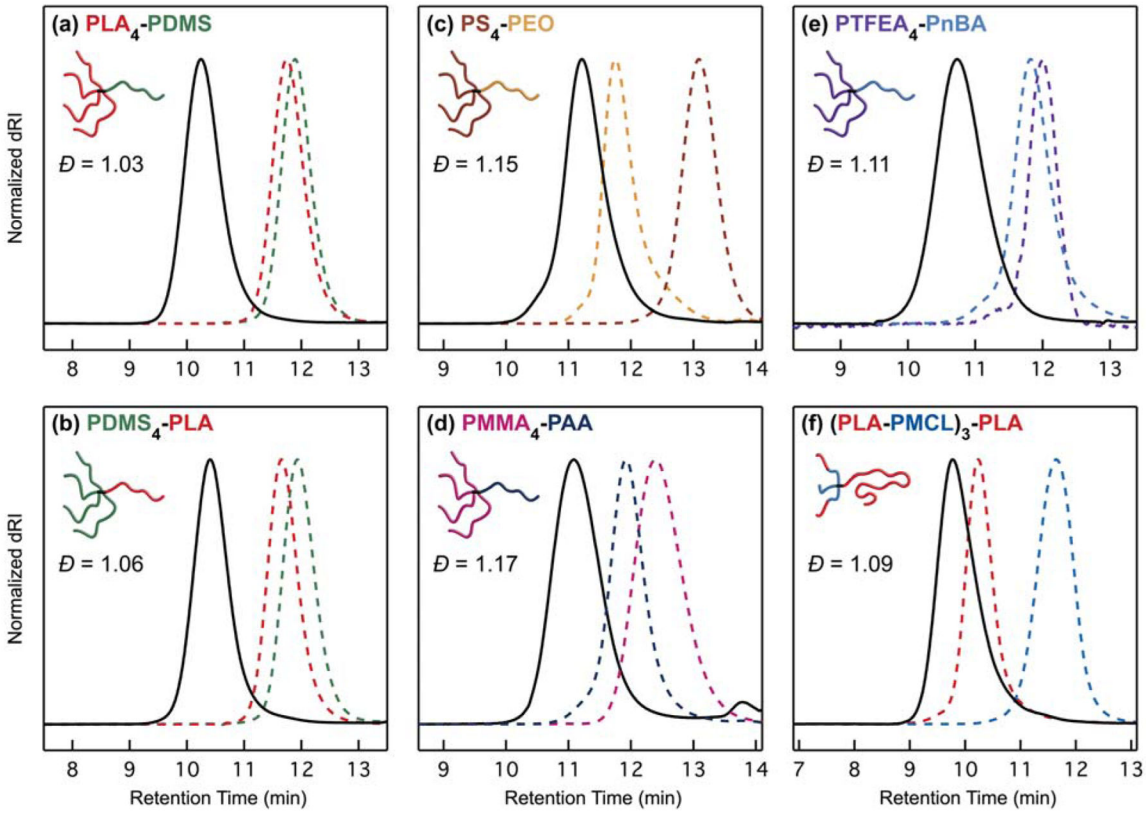

Figure 1.

Size-exclusion chromatograms (normalized differential refractive index signal, dRI) of the miktoarm star polymers (solid black lines) listed in Table 1. Macromonomers and macroterminators are depicted with dashed lines. See the Supporting Information (Figure S2–S10) for traces of the poly(macromonomers), which were omitted here for clarity. In (d), the macroterminator trace represents poly(tert-butyl acrylate) before deprotection, while the final miktoarm star curve comprises poly(acrylic acid) after deprotection. Also note that the small bump near 14 min is small molecule elution. In (e), the PTFEA macromonomer and PTFEA4-PnBA samples have negative dn/dc values in THF; the dRI data were multiplied by −1 for the purpose of consistent presentation.

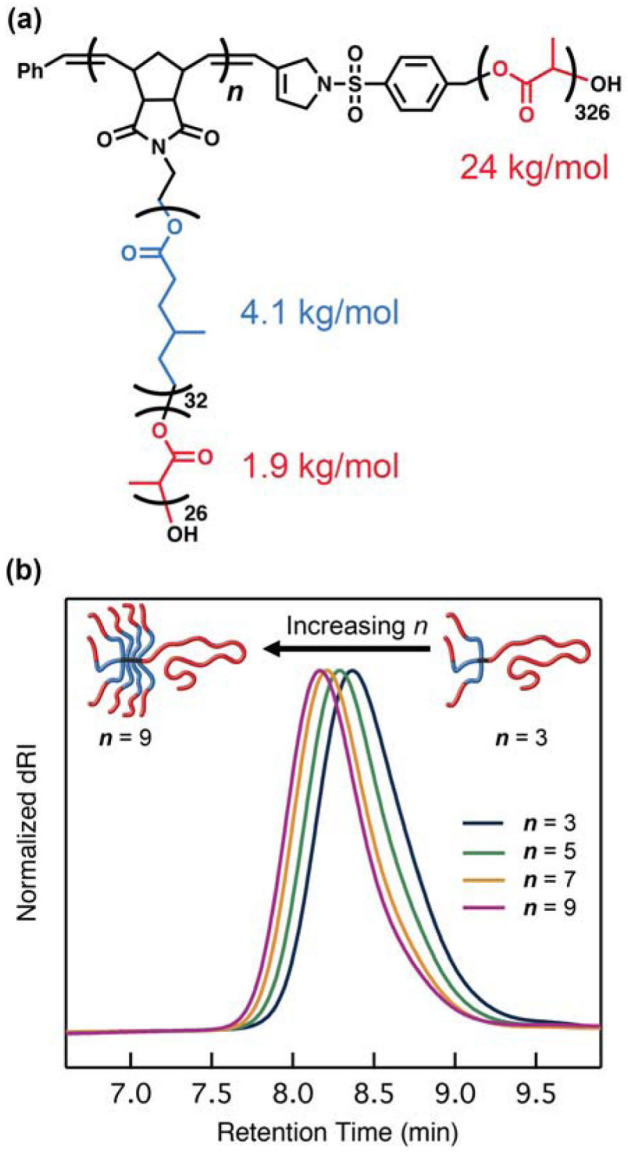

Figure 2.

μSTAR can easily vary the average number of arms n in an asymmetric miktoarm star polymer. (a) Chemical structure of (PLA-PMCL)n-PLA with n = 3 – 9. (b) Normalized differential refractive index signal from SEC analysis of the isolated miktoarm star polymers. See Table S4 for a summary of molecular weights and dispersities.

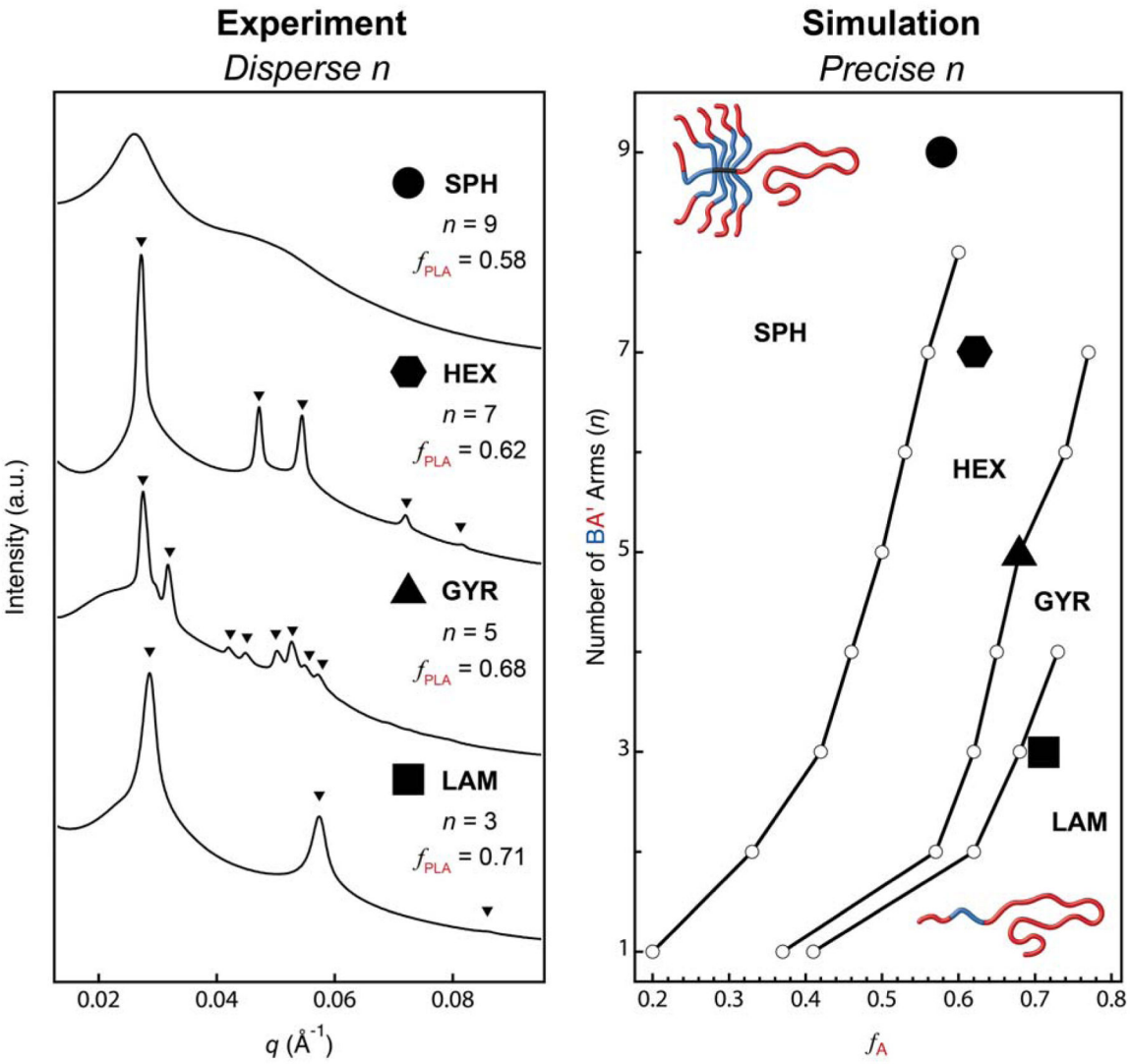

Figure 3.

The phase behavior of (PLA-PMCL)n-PLA miktoarm star polymers containing dispersity in n is consistent with simulations of precise analogues. (a) Small-angle X-ray scattering data with triangles demarcating the expected location of Bragg reflections for lamellar (LAM, n = 3), gyroid (GYR, n = 5), and hexagonally close-packed cylinder (HEX, n = 7) morphologies. (b) SCFT simulations at $\tau \equiv NA/(NA + NA') = 0.91$ relating morphology, PLA volume fraction (fPLA), and the number of PMCL-PLA (BA′) diblock arms (n) at $\chi N = 36$, which corresponds to the segregation strength at 298 K.76 Superposed symbols represent the four experimental samples from part (a).

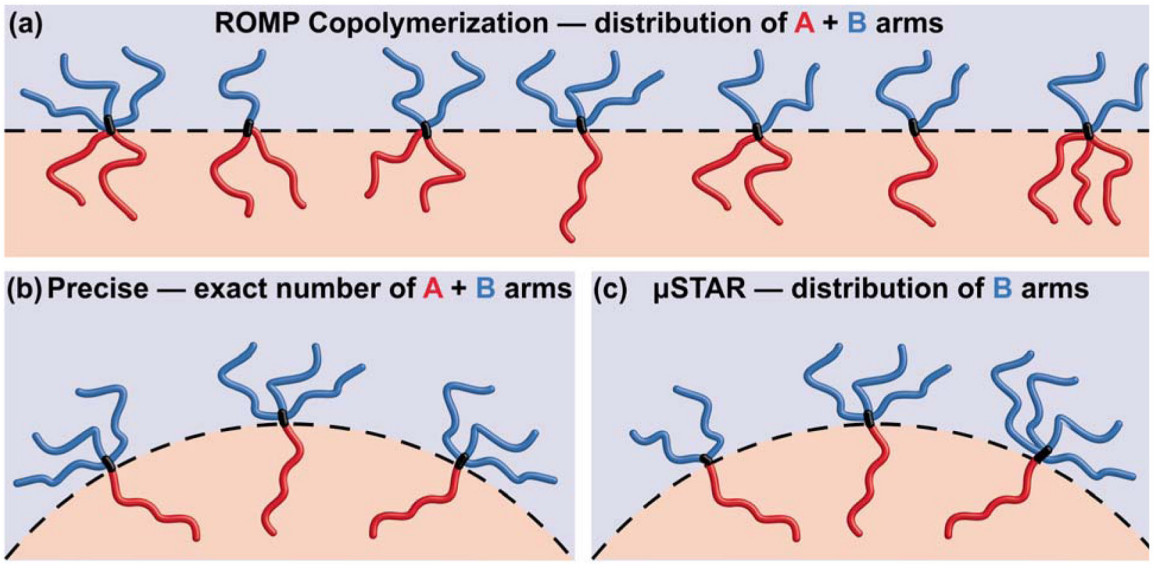

Figure 4.

Illustration of molecular composition and self-assembly resulting from different miktoarm star synthesis techniques. (a) Simple ROMP copolymerization of two macromonomers generates dispersity in composition and the number of A and B arms, which promotes flat block–block interfaces.58 (b) Asymmetric miktoarm stars (e.g., AB3) created by a precise synthesis favor interfacial curvature toward the A block.15 (c) μSTAR produces miktoarm stars with a distribution of B arms and exactly one A arm, resulting in interfacial curvature that is equivalent to precise analogues comprising the average molecular composition.

Table 1.

(top) Generic μSTAR synthesis of miktoarm star polymers using norbornene-functionalized macromonomers and enyne macroterminators. (bottom) Macromonomers, macroterminators, and miktoarm star polymers synthesized in this work.

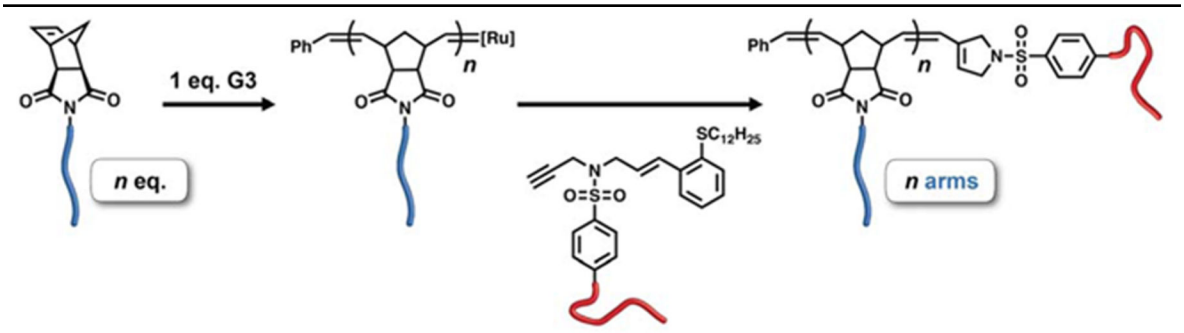

Macromonomer	Macroterminator	Miktoarm Star
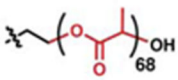	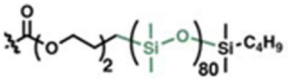	PLA_4-PDMS
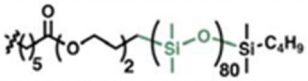	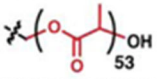	$PDMS_4$-PLA
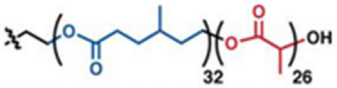	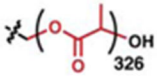	$(PLA\text{-}PMCL)_3$-PLA
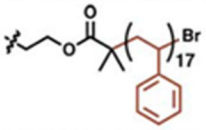	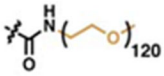	PS_4-PEO
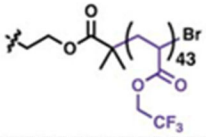	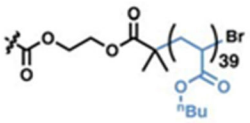	$PTFEA_4$-PnBA
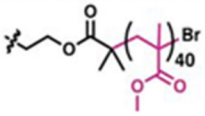	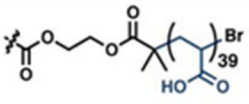	$PMMA_4$-PAA